Electron Transfer between a Photoexcited Azo Pigment Particle and an Electron Donor Molecule in a Solid System

Tatsuya Niimi[‡] and Minoru Umeda*[,†]

Imaging Technology Division, Ricoh Co., Ltd., 146-1 Nishisawada, Numazu, Shizuoka 410-0007, Japan, and Department of Applied Chemistry, Graduate School of Engineering, Tohoku University, Aramaki Aoba 07, Aoba-ku, Sendai 980-8579, Japan

Received: September 25, 2001; In Final Form: December 15, 2001

Carrier generation layer samples representative of layered photoreceptors consisting of carrier generation materials (CGM), carrier transport materials (CTM), and binder resin were prepared by the wet-coating technique. The samples were analyzed in terms of the CTM reaction species, the morphology of molecular contact at the CGM/CTM interface, and the CGM reaction species, all of which affect the photoinduced electron transfer (ET) in the samples. The ET reaction was found to be dependent on the CTM concentration through photoluminescence (PL) quenching in steady-state measurements. An analysis of this concentration dependence revealed that only the nearest CTM molecules to CGM particles participate in photoinduced ET. From the results of PL lifetime measurements, it was clarified that excitons near the surface of the CGM particles diffuse efficiently to the interface to participate in the reaction, whereas excitons near the center of the particles are deactivated before reaching the surface (reaction site).

1. Introduction

Light-to-electrical energy conversion in organic solids has attracted significant interest because the conversion efficiency in organic photoreceptors is greater than 0.5.[1] This is remarkable, even considering that photoreceptors are used in high external electric fields. The conversion efficiency is conventionally expressed[2] as the product of (i) the charge-separation efficiency for the formation of geminate hole−electron pairs and (ii) the geminate-pair dissociation efficiency into free carriers.

$$M_1^* + M_2 \rightarrow (M_1^- \cdots M_2^+) \rightarrow M_1^- + M_2^+ \qquad (1)$$

Here, M_1 and M_2 indicate organic molecules; in the case of intrinsic mechanisms, M_1 and M_2 are of the same kind, and in the case of extrinsic mechanisms, M_1 and M_2 are of different kinds.

Phthalocyanines[3] and azo pigments[4,5] are known to be highly photosensitive materials. In phthalocyanines, the first photoinduced electron transfer (ET)[6,7] occurs as an electric-field-dependent process at the location of photon absorption.[8] The first ET is the rate-determining step in overall carrier photogeneration and has already been treated theoretically.[9]

In contrast, photocarrier generation in the azo-pigment-based system is extrinsically sensitized by the electron-donor molecules involved.[10,11] This implies that photon absorption occurs in the azo pigment particle and that ET occurs at the interface between the pigment particle and the donor molecule.[12,13] The photoexcited exciton state is also known to migrate through the pigment particle to the interface. Therefore, geminate-pair promotion in the azo system is more complicated than that in phthalocyanines. Geminate-pair promotion in azo systems is electric-field-independent and is the rate-determining step in high electric fields.[11]

In a layered system, an azo pigment particle/donor molecule interface in the layered photoreceptor is formed as a result of intermingling when the azo-pigment-based layer is coated with the donor-molecule-based layer.[13] However, the photoinduced ET in the particle/molecule system that accompanies exciton diffusion is not adequately understood. The exciton diffusion has been known to occur in many organic compounds;[14−16] appreciation of the diffusion mechanism in the highly photosensitive azo-based photoreceptor is essential for the organic photoreceptor study.

In the present study, we form a single layer consisting of azo pigment, donor molecules, and binder resin, representing a photocarrier generation layer as appears in wet-coated photoreceptors.[17] We investigate the migration process and the interfacial ET, focusing on the reaction species of the azo molecules and donor molecules at the interface.

2. Experimental Section

The chemical structures of the fluorenone bisazo pigment, 4,4′-[(9-oxo-9*H*-fluorene-2,7-diyl)bis(azo)]bis[*N*-(2-chlorophenyl)-3-hydroxy-2-naphthalenecarboxamide] (carrier generation material, CGM),[18] and the donor molecule, 4-(2,2-diphenylethenyl)-*N*,*N*-bis(4-methylphenyl)benzenamine (carrier transport material, CTM),[19] used in this study are given in the inset of Figure 1. A cyclohexanone dispersion containing polyvinyl butyral (PVB) and CGM at a weight ratio of 4:10 was prepared using a ball mill. The dispersion was applied to a quartz glass plate by dip-coating to form a carrier generation layer (CGL). Another sample was prepared in the same manner using a CGM dispersion containing dissolved CTM. The CGM-based layer was fabricated such that the maximum absorbance of the layer at 583 nm is 1.0 and then dried for 10 min at 120 °C in an air atmosphere unless otherwise stated. A tetrahydorofuran (THF) solution containing bisphenol A−polycarbonate (PC) and CTM at a weight ratio of 10:9 was applied in the same manner to form a carrier transport layer (CTL) with a thickness of 0.3 μm.

* To whom correspondence should be addressed.
‡ Ricoh Co., Ltd..
† Tohoku University.

10.1021/jp013614e CCC: $22.00
Published on Web 03/14/2002

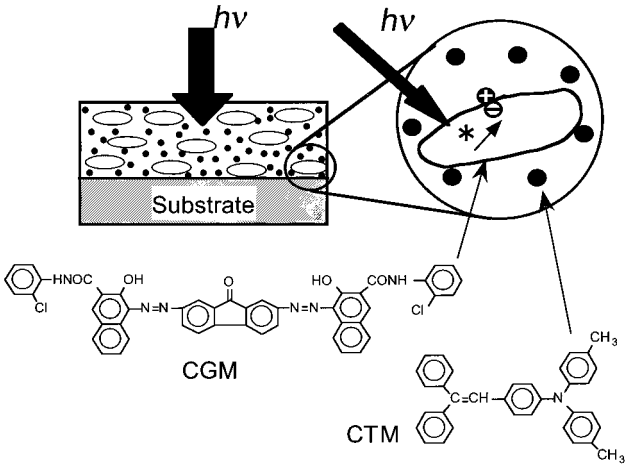

Figure 1. Schematic of photoinduced electron transfer at the CGM/CTM interface in CTM-doped CGL, which is representative of CGL in dual-layered organic photoreceptors produced by wet coating. The asterisk (∗) denotes photoexcited CGM. The chemical structures of CGM and CTM are also shown.

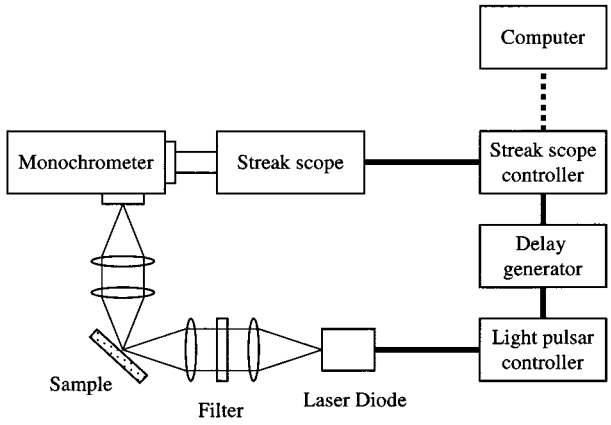

Figure 2. Schematic diagrams of experimental apparatus for CGM PL lifetime measurement.

The photoluminescence (PL) spectra of CGM were measured using an intensifier multichannel photodetector (Otsuka Electronics, IMUC-7000) with a He−Ne laser (632.8 nm, 1.4 mW) excitation source.[11] The photodetector for this steady-state measurement of PL spectra was a photodiode array in combination with an image intensifier tube. The photodetector was protected from the exciting light by a 650-nm short-wavelength cutoff filter. CGL luminescence was measured in the range 650−900 nm with a sampling time of 200 ms, and the data were integrated eight times to improve the signal-to-noise (S/N) ratio.

Absorption spectra were measured in the range 300−800 nm using a spectrophotometer (Shimadzu, UV-3100). The photoluminescence (PL) spectrum of CTL was measured in the range 400−700 nm using a fluorescence spectrophotometer (Hitachi, Ltd., F-3000).

The PL lifetime of CGM was measured using a picosecond fluorescence lifetime measurement system (Hamamatsu Photonics, C4780) with integrated streak camera (Hamamatsu Photonics, C4334) and laser diode (635 nm, 52.1 mW), for which the sample was excited for 71.6 ps at 1 kHz pulse frequency. The photodetector was protected from the exciting light by a 660-nm short-wavelength cutoff filter (Figure 2).

The thickness of samples was measured with a surface profile measuring system (Sloan, Dektak IIA). All measurements were conducted at room temperature.

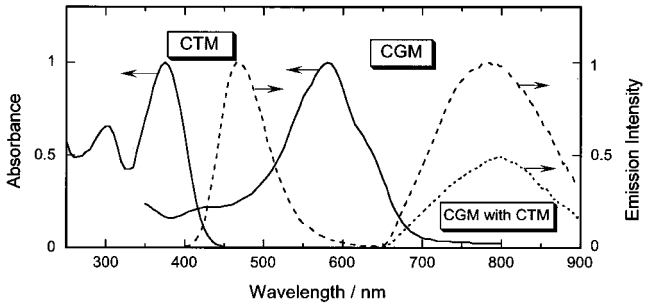

Figure 3. Absorption spectra (solid curves) and PL spectra (dashed curves) for single-layer 0.15-μm CGL (o.d. = 0.55) and single-layer 0.3-μm CTL. Dotted curve was a PL spectrum of the CGM-based layers doped with CTM (CTM/CGM = 1:1). The PL spectra of the CGL and CTL were obtained at excitation wavelengths of 632.8 and 370 nm, respectively. CGM primary particles have about a 0.1 μm major axis and about a 0.01 μm minor axis.

3. Results and Discussion

3.1. Photoinduced ET in a Single Layer Incorporating CGM, CTM, and Binder Resin. Figure 1 shows a schematic cross section of the sample coated on the substrate. Because the CTM and binder resin used here form a solid solution (molecularly doped polymer, MDP) at a random ratio,[20] the single-layered film separates into two phases: CGM particles and MDP, as shown in Figure 1.

Figure 3 shows the absorption and PL spectra for CGL (CGM/PVB = 10:4) and CTL (CTM/PC = 9:10). This figure also shows the PL spectra for the CGM sample containing CTM-doped CGL (CGM/CTM = 1:1). It is clear that the excitation light (632.8 nm) does not excite the CTM during measurement. All CGM-based samples have similar PL profiles. However, the CTM in CTM-doped samples clearly causes PL quenching of CGM. This PL quenching has been shown to occur as a result of ET from the highest occupied molecular orbital (HOMO) level of CTM at the ground state to the HOMO level of photoexcited CGM.[11]

From the above results, it is understood that the photoinduced ET in this system involves a process in which excitons generated from photoexcited CGM particles are transferred at the interface between CGM particles and CTM molecules, as shown in Figure 1. PL quenching by such ET represents a competitive reaction between the electron-transfer reaction and the deactivation reaction of the excited state, as given by

$$\mathrm{CGM^*} + \mathrm{CTM} \underset{k_{-d}}{\overset{k_d}{\rightleftharpoons}} (\mathrm{CGM^*\cdots CTM}) \xrightarrow{k_{et}} (\mathrm{CGM^-\cdots CTM^+}) \rightarrow \text{product} \quad (2)$$

$$\mathrm{CGM^*} \xrightarrow{k_L} \mathrm{CGM} \quad (3)$$

where CGM* is the photoexcited state of CGM, (CGM*···CTM) is the initial state of ET, ($CGM^-\cdots CTM^+$) is the geminate pair, and "product" is the recombined geminate pairs and the free carriers, k_d and k_{-d} are the initial state of ET formation and reverse rate constants. Equation 2 can be simplified as follows:

$$\mathrm{CGM^*} + \mathrm{CTM} \xrightarrow{k_s} (\mathrm{CGM^-\cdots CTM^+}) \quad (2')$$

3.2. Characterization of Donor Molecules That Participate in ET. Figure 4 shows the PL spectrum of the CTM-doped single-layer CGM sample. The PL intensity attributable to CGM decreases as the CTM content increases. From the PL maximum

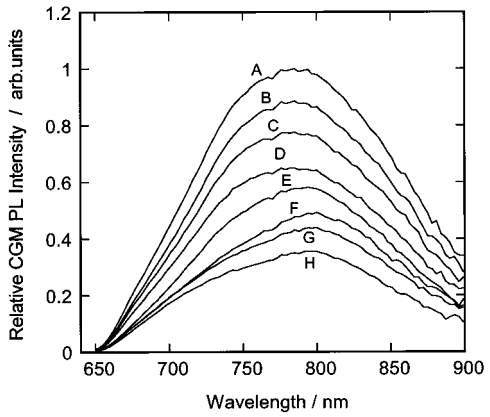

Figure 4. Photoluminescence spectra of the CGM-based layers doped with CTM as a function of CTM-doping quantity. CTM contents are (A) 0, (B) 0.7, (C) 2.1, (D) 6.7, (E) 26.3, (F) 41.7, (G) 51.7, and (H) 78.1 wt %. Excitation light intensity is 1.4 mW at 632.8 nm.

shift from 785 to 797 nm with the added CTM, the quenching occurs in the short wavelength. This indicates that the excited state of CGM having higher energy selectively participates in the ET reaction. As the CTM concentration has a clear CGM PL quenching effect, the quenching dependence of CTM concentration was analyzed quantitatively.

From eqs 2′ and 3, the efficiency of charge separation (ϕ_s) involving the ET can be defined as

$$\phi_s = \frac{k_s[A^*][D]}{k_L[A^*] + k_s[A^*][D]} = 1 - \frac{\phi_{L2}}{\phi_{L1}} \tag{4}$$

where, ϕ_{L1} and ϕ_{L2} are the PL quantum efficiency of the non-CTM-doped CGM sample and the CTM-doped CGM sample, respectively, k_s is the reaction rate constant of overall ET, and k_L is the total sum of deactivation rate constants of the photoexcited CGM and is defined by $k_L = k_{ra} + k_{nr} + k_{isc} + ...$, where k_{ra} is the radiative transition (PL), k_{nr} is the nonradiative transition and k_{isc} is the reaction rate constant for the intersystem crossing. [A*] and [D] are the concentrations of excited CGM and CTM participating in the reaction, respectively.

For the ET reaction, eq 4 can be modified to a Stern−Volmer equation,

$$\phi_s^{-1} = 1 + \frac{k_L}{k_s}[D]^{-1} \tag{5}$$

The effect of CTM concentration, [D], on ET can now be discussed in relation to eq 5. The CTM-doped single-layered CGL sample can be assumed to be a phase-separated structure in which a uniform MDP phase composed of CTM and PVB is segregated from CGM particles. The CTM concentration participating as a reactive species can therefore be regarded as only the concentration in the MDP phase.

In amorphous molecularly doped polymers, in this case CTM and polymer, the intermolecular distance R is commonly defined in terms of the CTM concentration. The following relation has been developed in carrier transport studies.[22,23]

$$R = \left(\frac{M}{N_A \rho x}\right)^{1/3} \tag{6}$$

where M is the molecular weight of CTM (451), N_A is Avogadro's number, ρ is the specific gravity of the product (1.15), and x is the CTM content.

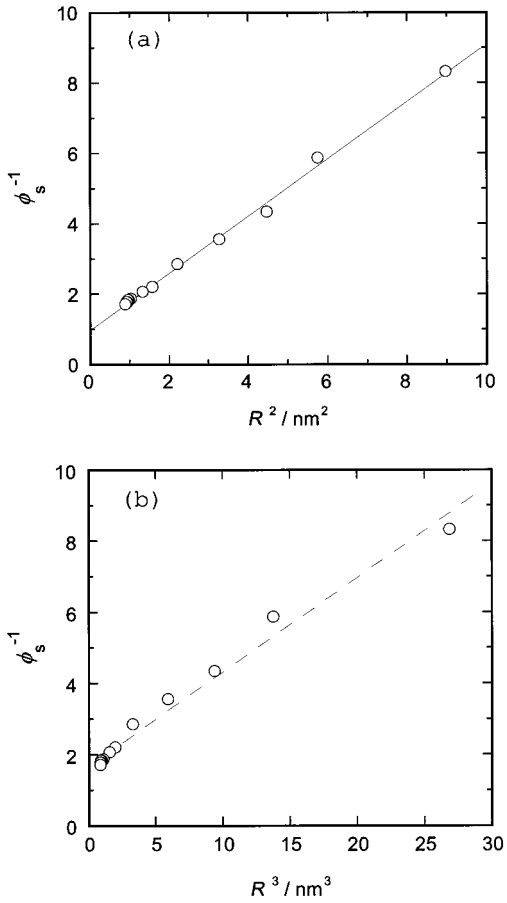

Figure 5. Reciprocal overall ET efficiency versus (a) squared intermolecular distance between CTMs and (b) cubed intermolecular distance between CTMs.

Two likely models can be proposed for the value [D] in eq 5. In the case where only nearest-neighbor CTMs react with the CGM particle, [D] will reflect the CTM concentration at the interface, given by R^{-2}. On the other hand, in the case where CTMs can react irrespective of the distance from the CGM particles, [D] will reflect the bulk concentration, given by R^{-3}.

Figure 5a shows the relationship between (i) the reciprocal ET efficiency obtained from the PL quenching results in Figure 4 and (ii) the square of the intermolecular distance, representing the reciprocal CTM concentration at the interface. The points fall on a straight line that passes through the point (0,1), corresponding to eq 5. In contrast, the points in Figure 5b, plotting R^3 instead of R^2, neither fall on a straight line nor pass through the (0,1) point. This suggests that photocarrier generation occurs between CGM and CTM adjacent to the surface of the CGM particle, as shown schematically in Figure 1.

3.3. Characterization of CGM Molecules That Participate in ET. Figure 6a shows the time decay curves for PL intensity from the CTM-free CGM sample together with those for the excitation laser beam and the fitting curves. Fitting is successful using the one-component analysis defined by the following equation:

$$I'_{L1}(t) = A \exp\left(\frac{-t}{\tau}\right) \tag{7}$$

where, A is a coefficient and τ is the PL lifetime.

Figure 6b shows the same results for the CTM-doped sample. In this case, fitting was successful using the two-component analysis defined by eq 8. For all CTM-doped samples, inde-

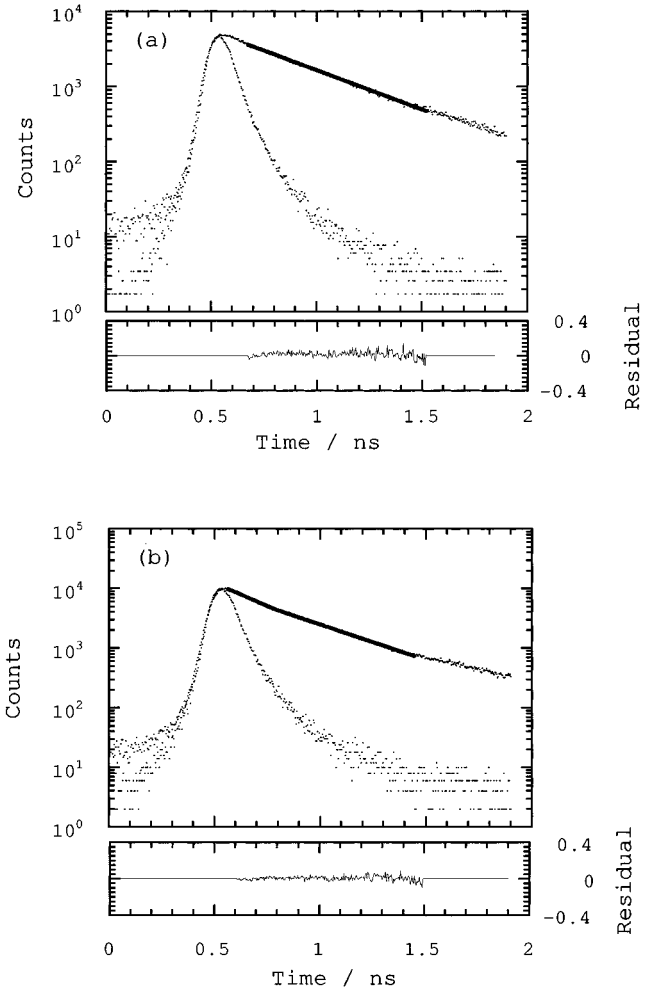

Figure 6. Decay profiles of PL from (a) single CGL and (b) CGM-based layers doped with CTM (CTM/CGM = 1:1). The data points (circles) are observed decay and the solid curves are one-component fitting for single-CGL and two-component fitting for CGM-based layers doped with CTM. The excited light pulse response is also presented by the dot. The lower graphs show the weighted residuals after curve fitting.

pendent of the doping quantity, the two-component analysis was successful.

$$I'_{L2}(t) = A_1 \exp\left(\frac{-t}{\tau_1}\right) + A_2 \exp\left(\frac{-t}{\tau_2}\right) \tag{8}$$

Table 1 lists all of the fitting parameters that were examined. The goodness-of-fit parameter χ^2 of 1.1 and 1.31 indicates that the data shown in Table 1 are reliable.[24] Here, the lifetime of the long-life PL component of the CTM-doped sample is in good agreement with the lifetime of the PL component for the non-CTM-doped sample. The existence of a two-component PL lifetime has been observed in the intermolecular photoinduced ET between donors and acceptors and has been described by the coexistence of two solid conformations: one in which electron transfer occurs and the other in which no electron transfer occurs.[25,26] Two lifetimes shown in Table 1 are considered to result from rapid quench of excitons near the surface participated in the CTM ($\tau_1 \approx 40$ ps) and nonquench of excitons in the bulk ($\tau_2 \approx 400$ ps). In the present system, it is assumed that excitons generated near the CGM particle surface are allowed to react with CTM molecules at the interface and that excitons inside the CGM particle are prevented from reaching the surface by diffusion and are deactivated (rate-determining process). The following relationships between τ_1, τ_2, ϕ_{L2}, and ϕ_{L1} then hold:

TABLE 1: List of Fitting Parameters and Calculated ϕ'_s

CTM/CGM	τ_1 (ps)	A_1	τ_2 (ps)	A_2	χ^2	ϕ'_s
0			415.72 ± 3.29	0.037	1.3002	
0.01:1	32.16 ± 0.29	0.075	434.25 ± 2.33	0.029	1.1085	0.668
0.02:1	41.99 ± 0.41	0.038	410.96 ± 1.16	0.034	1.1372	0.474
0.03:1	49.77 ± 0.29	0.043	435.41 ± 1.16	0.029	1.2739	0.529
0.05:1	33.77 ± 0.29	0.075	416.78 ± 1.16	0.034	1.3064	0.632
0.1:1	43.66 ± 0.29	0.044	416.78 ± 1.16	0.031	1.2333	0.525
0.2:1	35.61 ± 0.21	0.069	400.49 ± 0.58	0.032	1.2926	0.622
0.3:1	50.06 ± 0.21	0.036	392.67 ± 3.29	0.030	1.2688	0.476
0.5:1	41.22 ± 0.15	0.048	389.38 ± 3.29	0.026	1.2234	0.580
0.75:1	37.33 ± 0.29	0.058	366.33 ± 3.29	0.030	1.2690	0.592
1:1	46.20 ± 0.41	0.042	366.33 ± 3.29	0.029	1.1312	0.517
2:1	48.67 ± 0.41	0.045	363.03 ± 3.29	0.027	1.1871	0.541
5:1	73.88 ± 0.41	0.029	349.86 ± 1.65	0.031	1.2990	0.381

$$\phi_{L2} = k_{ra}\tau_1 \tag{9}$$

$$\phi_{L1} = k_{ra}\tau_2 \tag{10}$$

The emission intensity is defined by

$$I'_{L1} = CN\phi_{L1} \tag{11}$$

$$I'_{L2} = CN(A_1\phi_{L2} + A_2\phi_{L1}) \tag{12}$$

where, I'_{L1} and I'_{L2} are the PL intensity of the non-CTM-doped CGM sample and the CTM-doped CGM sample, respectively, N is the incident light intensity, and C is a constant of proportionality.

Here, the charge-separation efficiency in the PL lifetime measurement (ϕ'_s), which is obtained by substituting eqs 9−12 for eq 4, is expressed as follows:

$$\phi'_s = 1 - A_2 - A_1\left(\frac{\tau_1}{\tau_2}\right) \tag{13}$$

Table 1 lists ϕ'_s values calculated by eq 13 from the PL lifetime. Here, ϕ'_s is independent of CTM concentration, which differs from the results obtained by the steady-state measurement in Figure 5.

On the basis of this information, the reaction order of the charge-separation rate for CTM can be determined.

$$\frac{I_{L2}}{I_{L1}} - 1 = \frac{k_s[A^*][D]}{k_L[A^*]} = \frac{r_S}{r_L} \tag{14}$$

where I_{L1} and I_{L2} are the PL intensity of the non-CTM-doped CGM sample and the CTM-doped CGM, respectively.

This equation represents the ratio of the charge-separation rate, r_S, to the deactivation rate, r_L. Values for the left-hand side of eq 14 from (i) steady-state and (ii) PL lifetime measurements are plotted with respect to CTM concentration in Figure 7. Note that R^{-2} is used instead of CTM concentration, [D]. The logarithmic slopes of the two sets of data (steady-state and PL lifetime) are 1 and 0, respectively. The ET reaction is a bimolecular reaction as shown eq 4. In Figure 7, the result of r_S, which is proportional to the first power of the CTM concentration in the steady-state measurement, indicates that the photoexcited CGM concentration participated in ET reaction is sufficiently large. On the other hand, the result of r_S, which is independent of the CTM concentration in the PL lifetime measurement, shows that the CTM concentration is an excess (the photoexcited CGM concentration is insufficient). Conse-

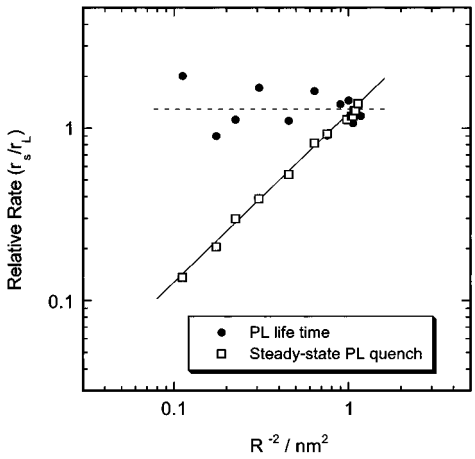

Figure 7. Logarithmic plot of the order of the reaction in terms of CTM concentration.

quently, the result of Figure 7 indicates that the exciton diffusion process cannot follow the ET reaction for about 40 ps. The result of Figure 7 also designates that the excitons near the surface of the CGM particles diffuse efficiently to the interface to participate in the ET reaction, whereas excitons near the center of the particles are deactivated before reaching the surface (could not participate in the ET).

The reaction rate constant k_s of the overall ET defined by eq 2′ can be rewritten as follows:

$$k_s = \frac{k_d k_{et}}{(k_{-d} + k_{et})} \tag{15}$$

The fact that the reaction rate of the overall ET is proportional to the first power of the CTM concentration in the steady-state measurement indicates that the experimental condition, in which [A*] is sufficiently large, is satisfied. In other words, ET is the rate-determining step ($k_{-d} \gg k_{et}$), and eq 15 is given by $k_s = K_d k_{et}$, where $K_d = k_d/k_{-d}$. Therefore, it is inferred that the diffusion process is in the preequilibrium state in reference to ET. That is, excitons in the CGM molecules that are capable of participating in reaction can be considered to diffuse at a sufficiently high rate.

Conversely, the fact that the reaction rate of the overall ET is independent of CTM concentration in the PL lifetime measurement indicates that the experimental condition ([A*] sufficiently large) is not satisfied, indicating that CTM molecules at the interface react with the excitons that diffuse to the surface. In other words, the rate-determining step ($k_{-d} \ll k_{et}$) is the diffusion of excitons, and eq 15 becomes $k_s \cong k_d$. This CTM-concentration independence of the quantum efficiency of the overall ET clearly indicates that a certain amount of excitons in the CGM particles always participate in the reaction, while other excitons do not. Consequently, it was clarified that the excitons near the surface of the CGM particles diffuse efficiently to the interface to participate in the ET reaction shown in Figure 1, whereas excitons near the center of the particles are deactivated before reaching the surface (reaction site).

4. Conclusions

Ternary-system CGL samples representing layered photoreceptors, consisting of a CGM (azo pigments), a CTM, and a binder resin, were prepared by the wet-coating technique. The samples were investigated in terms of the CTM reactive species, the CGM/CTM interface, and the CGM reactive species, all of which affect photoinduced ET in the samples. The photoinduced ET at the organic heterointerface of CGM particles and CTM molecules was found to be dependent on the CTM concentration through PL quenching in steady-state measurements. An analysis of this CTM-concentration dependency revealed that only the nearest CTM molecules to CGM particles participate in photoinduced ET; other CTM molecules do not participate in the reaction. On the basis of the finding that exciton diffusion is the rate-determining step of the reaction according to PL lifetime measurements, it was also shown that excitons generated near the surface of the CGM particles diffuse efficiently to the interface to participate in the reaction, whereas excitons near the center of the particles are likely to be deactivated before reaching the surface.

References and Notes

(1) Borsenberger, P. M.; Weiss, D. S. *Organic Photoreceptors for Xerography*; Marcel Dekker: New York, 1998; Chapter 6.
(2) Borsenberger, P. M.; Weiss, D. S. *Handbook of Imaging Materials*; Marcel Dekker: New York, 1991; Chapter 9.
(3) Fujimaki, Y.; Tadokoro, H.; Oda, Y.; Yoshikawa, H.; Homma, T.; Moriguchi, H.; Watanabe, K.; Kinoshita, A.; Hirose, N.; Itami, A.; Ikeuchi, S. *Proceedings of the 5th NIP Congress*; Society for Imaging Science and Technology: San Diego, CA, 1989; p 37.
(4) Hashimoto, H. U.S. Patent No. 5317093 (CAS No. 82829-36-5)
(5) Murakami, O.; Uenaka, T.; Otsuka, S.; Aramaki, S.; Murayama, T. *Proceedings of the 7th IS&T NIP Congress*; Society for Imaging Science and Technology: Portland, OR, 1991; Vol. 1, p 318.
(6) Fox, M. A.; Chanon, M. *Photoinduced Electron Transfer*; Elsevier: Amsterdam, 1988; Parts A−D.
(7) Kavarnos, G. J. *Fundamentals of Photoinduced Electron Transfer*; VCH Publishers: New York, 1993.
(8) Popovic, Z. D.; Menzel, E. R. *J. Chem. Phys*. **1979**, *71*, 5090.
(9) Lin, L.-B.; Jenekhe, S. A.; Borsenberger, P. M. *J. Chem. Phys*. **1996**, *105*, 8490.
(10) Umeda, M.; Shimada, T.; Aruga, T.; Niimi, T.; Sasaki, M. *J. Phys. Chem.* **1993**, *97*, 8531.
(11) Niimi, T.; Umeda, M. *J. Appl. Phys.* **1993**, *74*, 465.
(12) Umeda, M.; Hashimoto, M. *J. Appl. Phys*. **1992**, *72*, 117.
(13) Niimi, T.; Umeda, M. *J. Appl. Phys.* **1994**, *76*, 1269.
(14) Kao, K. C.; Hwang, W. *Electrical Transport in Solids*; Pergamon Press: Oxford, U.K., 1981.
(15) Rope, M.; Swenberg, C. E. *Electronic Processes Organic Crystals*; Oxford University Press: New York, 1982.
(16) Perlstein, J. H.; Borsenberger, P. M. In *Extended Linear Chain Compounds*, 2nd ed; Miller, J. S., Ed.; Plenum Press: New York, 1982; p 339.
(17) Borsenberger, P. M.; Weiss, D. S. *Organic Photoreceptors for Imaging Systems*; Marcel Dekker: New York, 1993; Chapter 10.
(18) Hashimoto, M. *Electrophotography* **1986**, *25*, 230.
(19) Sasaki, M. (Ricoh) U.S. Patent 4892949, 1984; *Chem. Abstr*. **1984**, *100*, 112236w.
(20) Umeda, M.; Niimi, T. *Jpn. J. Appl. Phys*. **1994**, *33*, L1789.
(21) Umeda, M.; Niimi, T. *J. Imaging Sci. Technol*. **1994**, *38*, 281.
(22) Stolka, M.; Yanus, J. F.; Pai, D. M. *J. Phys. Chem*. **1984**, *88*, 4707.
(23) Mack, X.; Schein, L. B.; Peled, A. *Phys. Rev. B* **1989**, *39*, 7500.
(24) O'Connor, D. V.; Phillips, D. *Time-correlated Single Photon Counting*; Academic Press: London, 1985; Chapter 6.
(25) Siemiarczuk, A.; McIntosh, A. R.; Ho, T.-H.; Stillman, M. J.; Roach, K. L.; Weedon, A. C.; Bolton, J. R.; Connolly, J. S. *J. Am. Chem. Soc*. **1983**, *105*, 7224.
(26) Noda, S.; Hosono, H.; Okura, I.; Yamamoto, Y.; Inoue, Y. *J. Chem. Soc. Faraday Trans.* **1990**, *86*, 811.